

Long-Endurance Flight Testing Results for the UIUC-TUM Solar Flyer

Or D. Dantsker*, Mirco Theile[†] and Marco Caccamo[‡]

Technical University of Munich, Garching, Germany

The growing application space of Unmanned Aerial Vehicles (UAVs) is creating the need for aircraft capable of autonomous, long-distance, and long-endurance flights. The two main challenges are the limited power capacity of UAVs, as well as the adaptation to real-time detected stimuli, changing the course of the mission. The UIUC-TUM Solar Flyer addresses the aforementioned challenges by balancing power consumption and solar power generation, and therefore enabling on-board data processing for real-time mission adaptation. The 4.0 m (157 in) wingspan Solar Flyer was developed from commercial-of-the-shelf components, making it affordable for a wide variety of applications. This paper describes the long-endurance flight testing results of the UIUC-TUM Solar Flyer from the Summer and Fall of 2020. The two flights presented and discussed in the paper are an approximately 1 hour flight performed under near ideal conditions and an 8 hour flight under non-ideal (cloudy and windy) weather conditions.

Nomenclature

AGL	=	above ground level	MPPT	=	maximum power point tracker
BEMT	=	blade element momentum theory	PWM	=	pulse width modulation
COTS	=	commercial-off-the-shelf	RPM	=	rotations per minute
ESC	=	electronic speed controller	UAV	=	unmanned aerial vehicle
GaAs	=	gallium arsenide			
GNSS	=	global navigation satellite system	ϕ, θ, ψ	=	roll, pitch and heading angles
IMU	=	inertial measurement unit			

I. Introduction

In recent years, we have seen an uptrend in the popularity of UAVs driven by the desire to apply these aircraft to areas such as precision farming, infrastructure and environment monitoring, surveillance, surveying and mapping, search and rescue missions, weather forecasting, and more. Since the inception of unmanned aircraft, a key design driver and limiter has been the limited on-board energy storage, as it significantly constrains flight time and ultimately usability. Notably, the majority of the aforementioned applications require continuous collection and processing of visual data. The traditional approach for small size UAVs is to capture data on the aircraft, stream it to the ground through a high power data-link, process it remotely (potentially off-line), perform analysis, and then relay commands back to the aircraft as needed.¹⁻⁵ Given the finite energy resources found on board an aircraft (battery or fuel), traditional designs greatly limit aircraft endurance since significant power is required for propulsion, actuation, and the continuous transmission of visual data.

All the mentioned application scenarios would benefit by carrying a high-performance, embedded computer system to minimize the need for data transmission. The aircraft should be able to carry a high-performance embedded computer

*Researcher, Department of Mechanical Engineering, or.dantsker@tum.de

[†]Ph.D. Student, Department of Mechanical Engineering, mirco.theile@tum.de

[‡]Professor, Department of Mechanical Engineering, mcaccamo@tum.de

system that could perform all required computations online and only downlink final results, saving a significant amount of energy. Performing on-line, on-board computation also allows the aircraft's autopilot to adapt its mission to external stimuli in real-time, broadening the application space of UAVs. A major technical hurdle to overcome is that of drastically reducing the overall power consumption of these UAVs so that they can be powered by solar arrays, therefore extending flight time. When powered by solar arrays, a careful reduction in battery size can decrease the aircraft's weight, reducing propulsion power even further. An additional advantage of long-endurance flight is the increase in aircraft availability and the decrease of takeoffs and landings that constitute the riskiest portions of flight. Currently, all long endurance solar-powered aircraft have incorporated custom airframe designs and many custom components (e.g. single-application propellers and gearboxes, maximum peak power-point trackers, etc.)^{6,7} However, to truly enable the above applications, the solar-powered aircraft needs to be assembled from only commercial-off-the-shelf (COTS) components and that it can sustain continuous flight. Using only COTS components reduces aircraft cost, thereby increasing accessibility to the community.

Assuming the ambitious goals of on-board computing, long-endurance flight capabilities, and COTS-only components are achieved, the resulting unmanned aircraft will be more readily available to various communities such as research, industry, and emergency response, among others. For this purpose, a computationally-intensive, long-endurance solar-powered unmanned aircraft called the UIUC-TUM Solar Flyer⁸ was developed, which is shown in Fig. 1. The aircraft was built from a majority of COTS components using a mixture of trade studies and power simulations in order to enable a variety of all-daylight hour missions while minimizing aircraft size. The 4.0 m (157 in) wingspan UIUC-TUM Solar Flyer aircraft weighs approximately 3.3 kg (7.2 lb) and will soon have the continuous daylight ability to acquire and process high resolution imagery. The aircraft is instrumented with an autopilot and high-fidelity data acquisition system and is powered by a 64 W gallium arsenide (GaAs) solar array. Its configuration, wing platform area, and expected lift-to-drag ratio were also considered, along with motor and propeller data. This paper describes recent long-endurance flight testing performed with the UIUC-TUM Solar Flyer.

This paper first provides an overview of the UIUC-TUM Solar Flyer. This includes the development and testing that has occurred since project conception to date and the various tools and methodologies applied. Additionally aircraft and sub-system descriptions and specifications are provided. The paper then presents and discusses results from two long-endurance, solar-powered flights performed in the Summer and Fall of 2020. These flights include an approximately 1 hour flight performed under near ideal conditions and an 8 hour flight under non-ideal (cloudy and windy) weather conditions. Conclusions from these flight tests are then discussed. The paper ends with a statement of future work and application.



Figure 1: The flight-ready UIUC-TUM Solar Flyer aircraft.

II. Aircraft Overview

The UIUC-TUM Solar Flyer was developed to enable continuous, all-day acquisition and processing of high resolution visible and infrared imagery while minimizing resources. Systematic development efforts focused on optimizing the airframe, propulsion system, energy system, and avionics are described below. Final specifications of the aircraft are provided at the end of this section.

A. Airframe

A trade study was conducted to select a commercially-available airframe for the UIUC-Solar Flyer.⁹ A list of possible airframes was compiled and, using estimation methods, their performance was compared. Of the many commercial and hobby airframes available, the airframes considered had a high aspect ratio for high efficiency, a wingspan of greater than or equal to 3 meters, and be available at project start. This led to two manufactures: F5 Models,¹⁰ which previously provided airframes for other solar UAVs,^{11,12} and Top Model CZ.¹³ Estimations were made for solar power generation potential, based on available solar area, and for propulsion power requirements, based on airframe and other component mass, with efficiency reductions being accounted for both. The airframes were compared in terms of power available for the payload components as can be seen in Table 1.

Table 1: Comparison of possible airframes for the UIUC-TUM Solar Flyer.

Airframe	Wingspan [m]	Total Mass [gr]	Propulsion Power Required [W] $\eta = 50 - 65\%$	Solar Power Available [W]	Power Available for Components [W] $\eta = 50 - 65\%$
F5 Models Pulsar 4E	4.00	2310	36.3 – 27.9	66.3	30.0 – 38.4
F5 Models Pulsar 3.6E	3.60	2276	35.7 – 27.5	62.8	27.1 – 35.3
F5 Models Pulsar 3.2E	3.20	2167	34.0 – 26.2	55.0	21.0 – 28.8
F5 Models Pulsar Twin	3.00	2296	36.0 – 27.7	53.8	17.8 – 26.1
Top Model CZ Gracia MAXI	3.52	2480	38.9 – 29.9	62.5	23.5 – 32.5
Top Model CZ Gracia	3.07	2367	37.2 – 28.6	55.0	17.8 – 26.4
Top Model CZ Grafas MAXI	3.52	2480	38.9 – 29.9	62.5	23.5 – 32.5
Top Model CZ Grafas	3.07	2367	37.2 – 28.6	55.0	17.8 – 26.4
Top Model Samsara	3.20	2472	38.8 – 29.9	55.4	16.6 – 25.5
Top Model Thermik Dream	3.00	3008	47.2 – 36.3	47.5	0.3 – 11.2

The trade study yielded the choice of the F5 Models Pulsar 4E Pro. The Pulsar 4E also had the greatest wingspan and wing area while having one of the lowest non-instrumented, flight-ready mass. The Pulsar 4E fuselage is composed of a kevlar pod and a carbon fiber tail boom. All of the flight surfaces are built from balsa wood that is reinforced with carbon fiber and a kevlar-carbon fiber laminate. The wings are composed out of 3 sections: center with flaps and outer right and left with aileron. This allows for maximum solar power to be generated while minimizing the power required to propel the base airframe. The airframe was built per the manufacturer instructions with slight modifications to ease future computational device and solar array integration.

B. Propulsion System

Limited on-board energy availability significantly limits flight time and ultimately the usability of UAVs and the propulsion system plays a critical part in the overall energy power consumption of the UAV. Therefore, significant effort was put into the selection of propulsion system components on the UIUC-TUM Solar Flyer.^{14,15} Specifically, it was necessary to determine the most optimal combination of possible propulsion system components for a given mission profile, i.e., propellers and motors. Hundreds of options are available for each of the components with generally non-scientific advice for choosing the proper combinations. A fixed-wind, electric unmanned aircraft propulsion system power model¹⁶ and a mission-based propulsion system optimization tool¹⁴ were then developed to select the most optimal combinations of possible components, i.e., propellers and motors, for a given mission profile.

In order to optimize the UIUC-TUM Solar Flyer propulsion systems, performance parameters for potential motors and propellers were needed. As the propulsion system optimization tool uses a first order approximation¹⁷ for motor parameters, the parameters for potential motors could easily be obtained from the manufacturers. However, propeller performance and efficiency parameters could not be obtained as easily. Propeller performance can be derived using blade element momentum theory (BEMT) and sectional airfoil theory as performed in other work.¹⁸ However, BEMT curves are highly sensitive to variation of the parameters used. In order to increase model accuracy, experimental data for propeller performance had to be obtained from wind tunnel propeller testing¹⁹ as data for potential folding propellers was not available on existing databases. Thus, testing was performed for 40 Aero-Naut CAM carbon fiber folding propellers with diameters of 9 to 13" and a variety of pitches. The testing yielded thrust coefficient, power coefficient, and efficiency curves for a broad range of advance ratios at rotation rates between 3,000 and 7,000 RPM. The results are published on the UIUC Propeller Database²⁰ and the Unmanned Aerial Vehicle Database (UAVDB).²¹

The propulsion system optimization tool was then applied to a typical field coverage mission that the UIUC-TUM Solar Flyer would be expected to perform with all relevant aircraft parameters.²² The tool used the propeller performance data for 40 Aero-Naut CAM carbon folding propellers and motor parameters for 28 motors from Hacker Motor GmbH,²³ Model Motors s. r. o.,²⁴ and Neutronics,²⁵ which were mass and size compatible to the aircraft. 1120 combinations were computed and ranked by the efficiency. After considering thrust requirements for upset scenarios and thermal management, the Model Motors AXi 480/1380 and Aero-Naut CAM 12x8 were chosen as this combination provided a 15% increase in propulsion efficiency than the baseline combination and ample aircraft safety.

C. Energy Systems

The UIUC-TUM Solar Flyer energy systems were developed to collect, store, and distribute energy on-board as required. Gallium arsenide (GaAs) solar arrays from Alta Devices, which are estimated to be 25–26% efficient, are used on the aircraft in conjunction with a maximum power point tracking (MPPT) charge controller and a 3S 8P, 10.8V 28Ah Samsung 35E 18650 lithium-ion battery that acts as an energy buffer. The aircraft carries 64 W of solar cells mounted onto the upper surface of the wings; areas such as the leading edge and the control surfaces do not have solar cells mounted on them due to overhead weight and wiring associated as well as the decreased solar power production potential. The batteries are distributed within the fuselage, while maintaining center of gravity location. A side view of the fuselage layout is shown in Fig. 2

Initial testing was performed using a subset of 8W of solar arrays, a MPPT solar charge controller, and 3S, 10.8V 3.5Ah Samsung 35E 18650 lithium ion battery, which is 1/8 the capacity of the battery on the aircraft. The testing confirmed that solar power production is a function of the normalized dot product of the solar cell normal vector and the sun direction vector; this result was expected and allowed for the development of a solar production estimation model, that took into account aircraft attitude and location, time of day, and sun cover²⁶

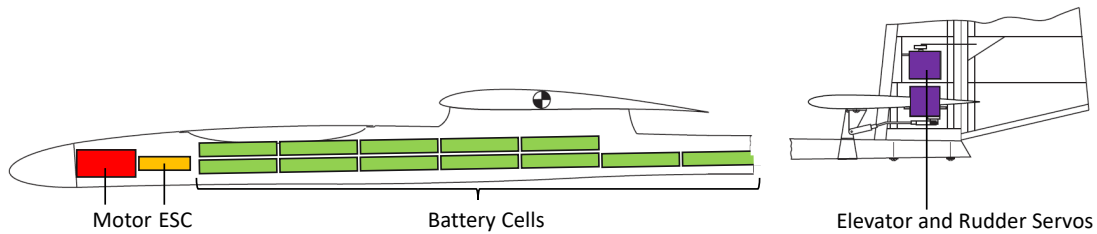


Figure 2: Side view of the UIUC-TUM Solar Flyer fuselage, showing the layout of the motor, the ESC, the battery cells, and the elevator and rudder servos.

D. Avionics

The UIUC-TUM Solar Flyer avionics are based around a commercially available flight control and data acquisition system, the Al Volo FC+DAQ,^{27,28} and uses the open-source uavAP autopilot^{29,30} and uavGS ground station interface.^{31,32} The system integrates a 9-DOF inertial measurement unit (IMU) and 10 Hz Global Navigation Satellite System (GNSS) and operates at 100 Hz. The main avionics unit as well as the airspeed probe and sensor, GNSS antenna, ESC data interface, 900 MHz radio module, and control multiplexer are laid out within the center wing panel; a top view of the instrumentation layout within the wing is shown in Fig. 3. Further detail regarding the UIUC-TUM Solar Flyer avionics development, and layout can be found in related literature.^{33,34}

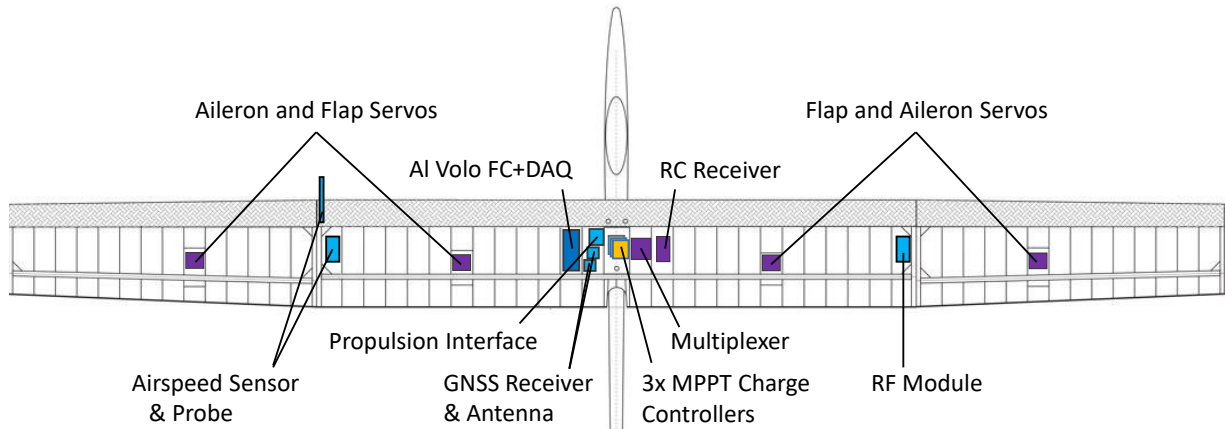


Figure 3: Top view of the UIUC-TUM Solar Flyer center and mid-outer wing sections, showing the layout of avionics components, MPPTs, and the aileron and flap servos.

E. Specifications

The physical and system component specifications of the UIUC-TUM Solar Flyer are provided below in Tables 2-5.

Table 2: Physical aircraft specifications of the UIUC-TUM Solar Flyer.

Geometric Properties	
Overall Length	1815 mm (71.5 in)
Wing Span	4000 mm (157.5 in)
Wing Area	85 dm ² (1318 in ²)
Aspect Ratio	18.8
Inertial Properties	
Empty Mass/Weight	2.0 kg (4.4 lb)
Battery Mass/Weight	1.3 kg (2.8 lb)
Gross Mass/Weight	3.3 kg (7.2 lb)
Wing Loading	39.1 gr/dm ² (12.8 oz/ft ²)

Table 3: Specifications of the UIUC-TUM Solar Flyer airframe, flight control, and propulsion systems.

Airframe	F5 Models Pulsar 4.0E
Flight Controls	
Receiver	Futaba R6208SB
Servos	(6) S3173SVi
Propulsion	
Motor	Model Motors AXi Cyclone 46/760
ESC	Castle Creations Phoenix Edge Lite 50
Propeller	Aeronaut CAM Folding 13x6.5

Table 4: Specifications of the UIUC-TUM Solar Flyer solar and energy storage systems.

Solar	
Photo Voltaic Cells	64W of Alta Devices Single Junction GaAS cells in 20S, 16P
Blocking & Bypass Diodes	80x Diodes Inc. 12A SBR
Charge Controller	Analog Devices MPPTs in 3P
Current Tracking	Allegro Hall-Effect Current Sensor
Energy Storage	
Battery	10.8V 28Ah Samsung 35E 18650 in 3S 8P

Table 5: Specifications of the UIUC-TUM Solar Flyer avionics.

Autopilot-DAQ system	Al Volo FC+DAQ 100 Hz flight control and data acquisition system
RF Module	Digi International 900 MHz XBee Pro S3B Module
Multiplexer	8-channel PWM multiplexer with redundant input
Sensors	
Inertial	100 Hz AHRS integrated into FC+DAQ
Positioning	10 Hz GNSS integrated into FC+DAQ
Airspeed sensor	Al Volo Pitot Static Airspeed Sensor
Motor sensor	Al Volo Castle ESC Interface
Power Regulator	Built into FC+DAQ

III. Flight Test Results and Discussion

In the Summer and Fall of 2020, the UIUC-TUM Solar Flyer performed several long-endurance, solar-powered flights. Two flights are presented below, which include an approximately 1 hour flight performed under near ideal conditions and an 8 hour flight under non-ideal (cloudy and windy) weather conditions. Note that the 1 hour flight occurred after the 8 hour flight, however, in order to better explain the effects of the non-ideal conditions to the 8-hour flight, the 1 hour flight under ideal conditions is presented first as a point of reference.

A. 1 Hour Flight under Ideal Conditions

An approximately 1 hour flight was performed on Oct 8, 2020 under ideal conditions. The UIUC-TUM Solar Flyer took off at 11:43 AM and landed at 12:40 PM local time. During that time the sun shifted from 42 deg elevation, and 158 deg azimuth to 45 deg elevation and 177 deg azimuth. A nearby national weather station reported that winds were calm to 3 mph (1.3 m/s) from a variable direction and that it was sunny with fair skies (less than 40% clouds). Locally at the field, the flight crew observed sunny skies with the winds of 3-5 mph (1.3-2.2 m/s) from the SSW (190-210 deg), which was aligned with the runway, from right to left (in the perspective of the flight crew).

The trajectory of the flight is shown in Fig. 4. The figure is laid out from the perspective of above the flight crew area, looking towards the flight testing area and the aircraft flight path. The takeoff was performed from the runway using a dolly, from left to right and was followed by an ascent into a clockwise race track flight pattern. Specifically, the aircraft was commanded to perform a race track pattern of 650×150 m at an altitude of 100 m AGL; and maintain an airspeed of 11 m/s. The aircraft performed 26 laps of the flight pattern with some deviations that are addressed below. This was followed by a descent to landing. The landing was performed from left to right, on a grass strip parallel to the runway.

The race track path flown is equivalent in flight maneuvering to an area coverage mission with 500 m long straights that are 150 m apart, with required 180 deg, 75 m radius turn-arounds at the ends of the straights. As mentioned, 26 laps were performed during the 53 min of maneuvering, yielding an effective coverage area of 1.95 km^2 (481 acre). Therefore, the race track maneuvering demonstrated equates to an area coverage of $2.2 \text{ km}^2/\text{hr}$ (545 acre/hr).

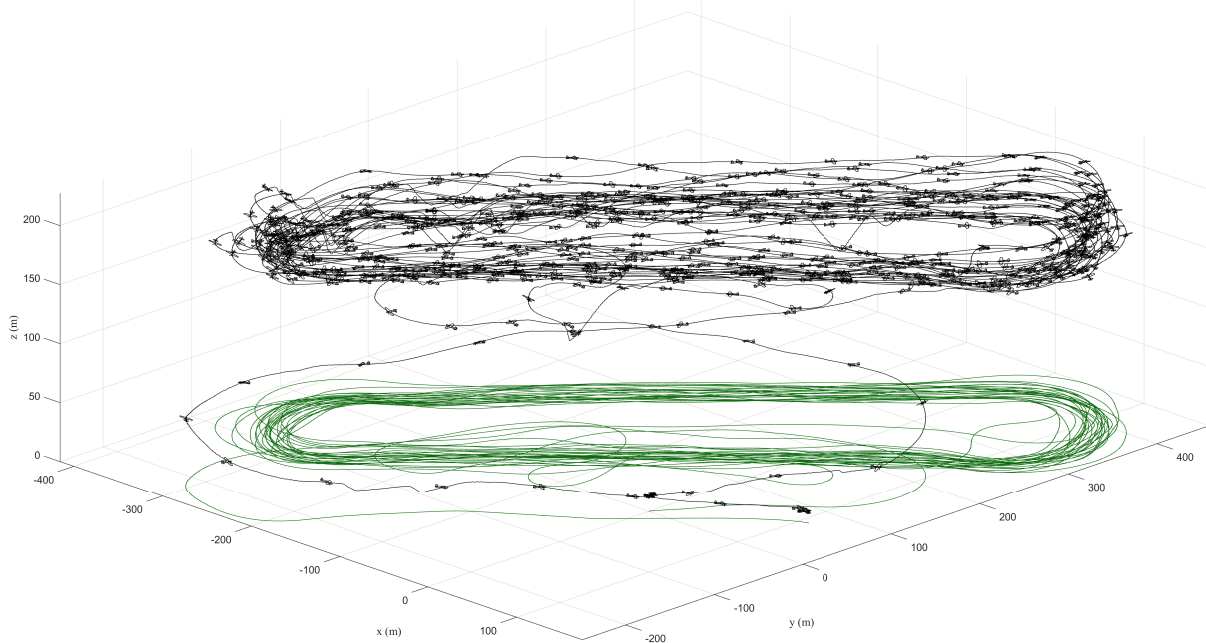


Figure 4: The trajectory of the UIUC-TUM Solar Flyer performing the approximately 1 hour flight under ideal conditions (note that the aircraft is plotted every 5 sec).

The state data time history is presented in Fig. 5. The Euler angle pitch and roll are presented in (a) and heading is presented in (b). The aircraft position, Northing and Easting, and the altitude are presented in (c) and (d), respectively; note that due to the flight site geography, the runway altitude is lower than the ground level of the maneuvering area yielding an altitude difference of greater than 100 m. The aircraft air and ground speeds are presented in (e); the ground speed is measured by the GNSS while the airspeed is computed by a wind-tunnel calibrated pitot-probe airspeed sensor. The propulsion power, measured at/between the battery and ESC, is presented in (f). The propeller rotation rate, measured by the ESC, is presented in RPM in (g). The battery voltage is presented in (h). And the solar power generated by the solar arrays is presented in (i).

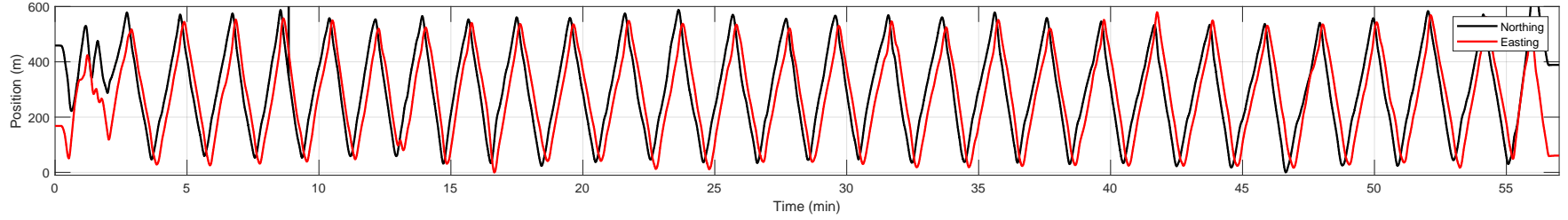
The position and Euler angle data shows 26 race track laps being performed, each approximately 2 min long. There are an increasing amount of mostly positive vertical excursions from the commanded altitude during the middle part of the flight. The airspeed data shows an attempt to maintain the 11 m/s commanded airspeed with increased airspeeds correlating to the times when the positive vertical excursions occurred. There are also a repeated offsets between air and ground speed, which result from wind; the magnitude is either positive or negative based on whether the aircraft is flying upwind or downwind.

The aircraft propulsion power heavily oscillates during the entire flight from 0 to 230 W. There is a decrease in the on-power times used during the middle of the flight when positive vertical excursions occurred; these are also the same times when the airspeed exceeded the commanded 11 m/s. In order to better estimate propulsion power consumption, 10 min moving averages of the race track laps were calculated, comprising of 5 laps of 60,000 data points each, yielding average power values between 14 and 53 W. Due to large difference in 10 min average values, a true average propulsion power consumption value could not definitively be calculated.

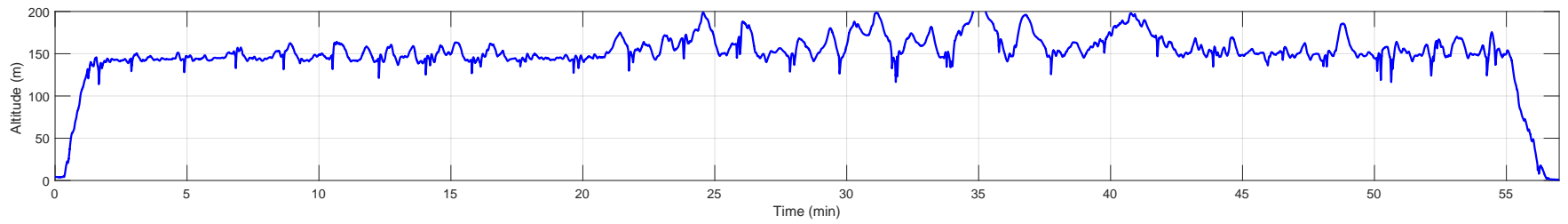
The propeller rotation rate correlates as expected with the propulsion power, i.e., when propulsion power is high, the propeller rotation rate increases to approximately 6,400 RPM, while when propulsion power is near 0, the propeller rotation rate decreases to approximately 2,900 RPM. This is indicative of the ESC throttling the motor on when the airspeed dips below 11 m/s and then off when it is above that airspeed. With the exception of an oscillation during takeoff, the battery voltage remains constant at 12.05 V. Finally the solar power varies cyclically between 14 and 55 W, correlating to the laps being performed; the average solar power was approximately 35 W.

In order to better assess the increasing altitude excursions, an 8 min portion of the flight, from 22 to 30 min, was visualized in Fig. 6 with the corresponding state data time history presented in Fig. 7. In general, the closer-in (right to left) straight leg, where the aircraft flies downwind, was relatively flat with minimal altitude deviations. However, the subsequent 180 deg turn and the first half of farther-out (right to left) straight leg, where the aircraft flew upwind, had consistent altitude deviations of up to 20-30 m. It is assumed that the uncommanded positive altitude deviations are the result of thermals. Meanwhile, the negative altitude deviations seem to be the result of an interplay between the autopilot attempting to pitch the aircraft downward to maintain altitude and the thermals weakening. In general, the far left area in the figure has consistently been reported by local pilots to be more turbulent, compared to other areas of the flying site. Observing the state data time history shows greater roll values in the left corner turn going into the farther-out upwind leg compared to the right corner turn going into the closer-in downwind left.

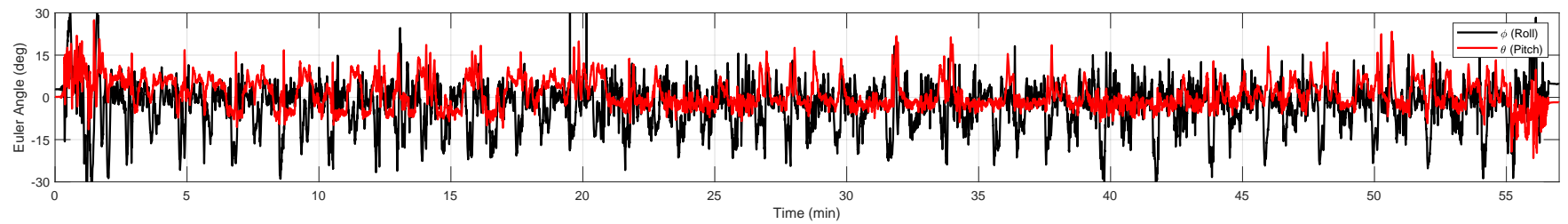
Additionally, observing the time history of the airspeed shows that in this portion of the flight, the airspeed only significantly dips below 11 m/s in turns, primarily in the turns from the upwind (farther-out) legs to the downwind (closer-in) legs. As a result, the ESC is commanded to throttle-up the motor to create thrust and increase airspeed, which corresponds to propulsion power consumption. During the remaining time in this flight portion, the ESC throttles the motor off with the propeller wind milling. The throttling-on and throttling-off of the motor is the result of the interplay between the autopilot and ESC controllers and limits. With the earlier thermal assumption, it is assumed that some of the energy used to propel the aircraft and counter drag also comes from thermals through the uncommanded altitude and thus potential energy gains – this seems evident from the rapid altitude gains followed by gradual, gliding descents.



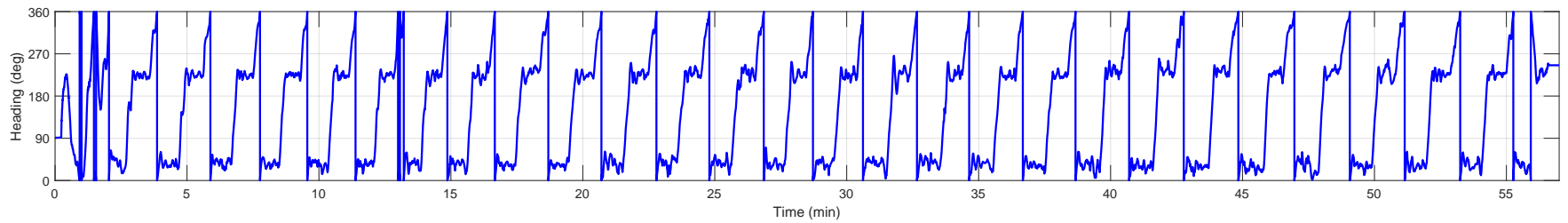
(a)



(b)

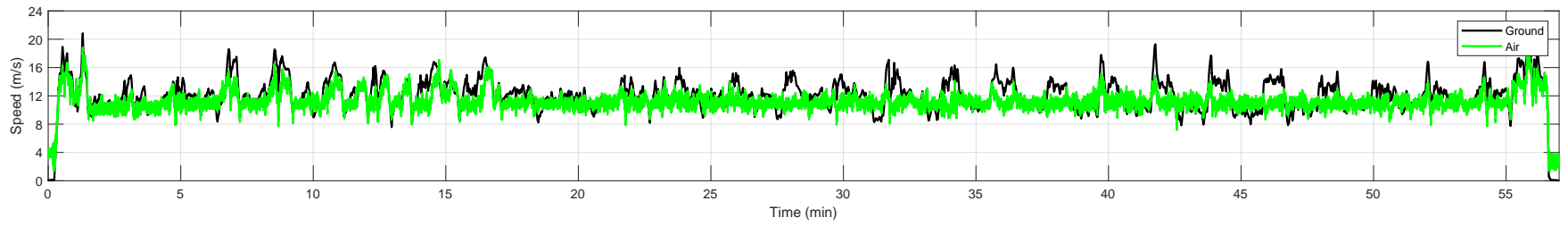


(c)

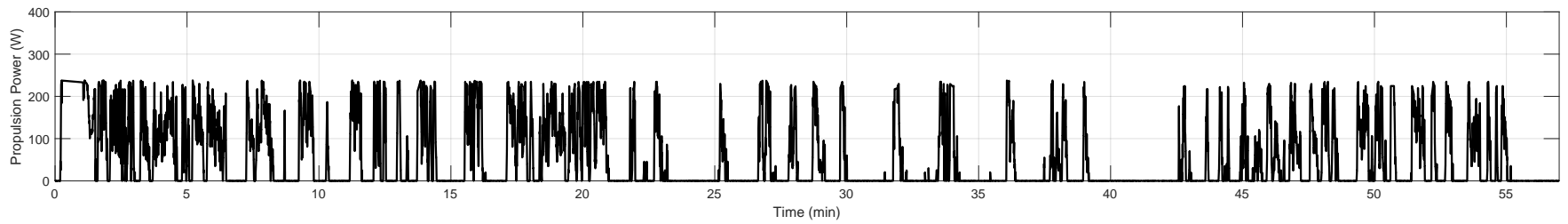


(d)

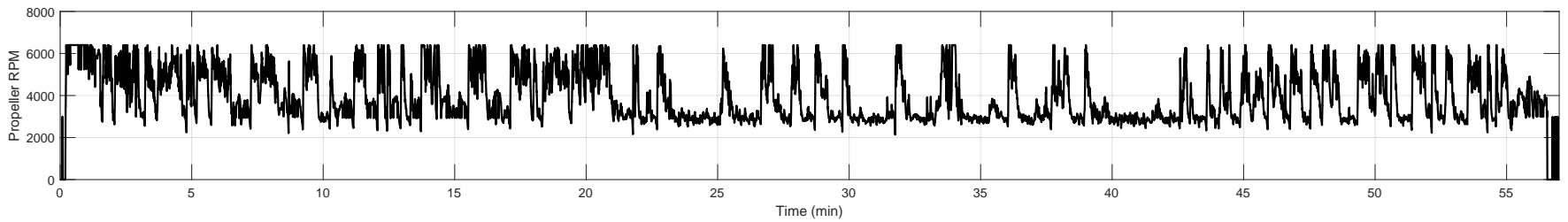
Figure 5: The state data time history of the UIUC-TUM Solar Flyer performing the approximately 1 hour flight under ideal conditions: (a) Northing and Easting position, (b) altitude, (c) pitch and roll, (d) heading.



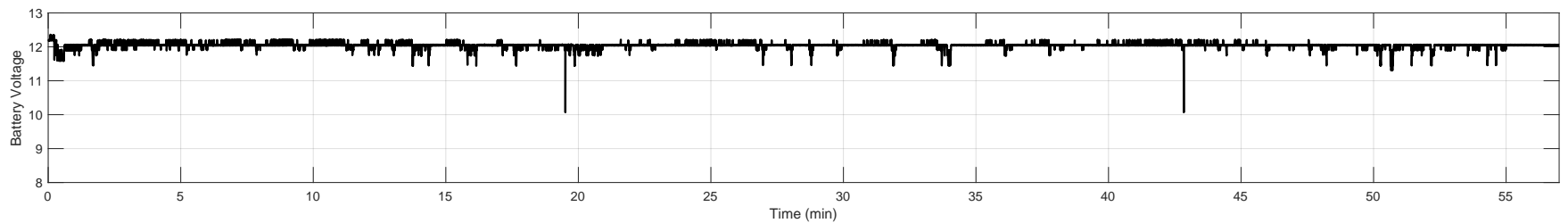
(e)



(f)

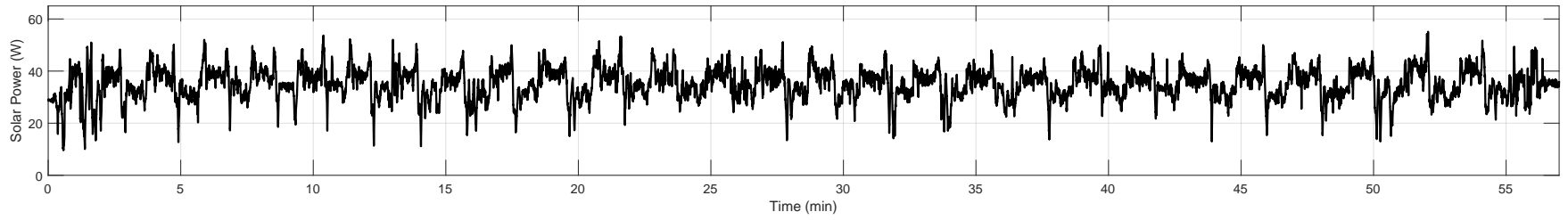


(g)



(h)

Figure 5 (continued): The state data time history of the UIUC-TUM Solar Flyer performing the approximately 1 hour flight under ideal conditions: (e) air and ground speed, (f) propulsion power consumption, (g) propeller rotation rate in RPM, (h) battery voltage.



(i)

Figure 5 (continued): The state data time history of the UIUC-TUM Solar Flyer performing the approximately 1 hour flight under ideal conditions: (i) solar power generated.

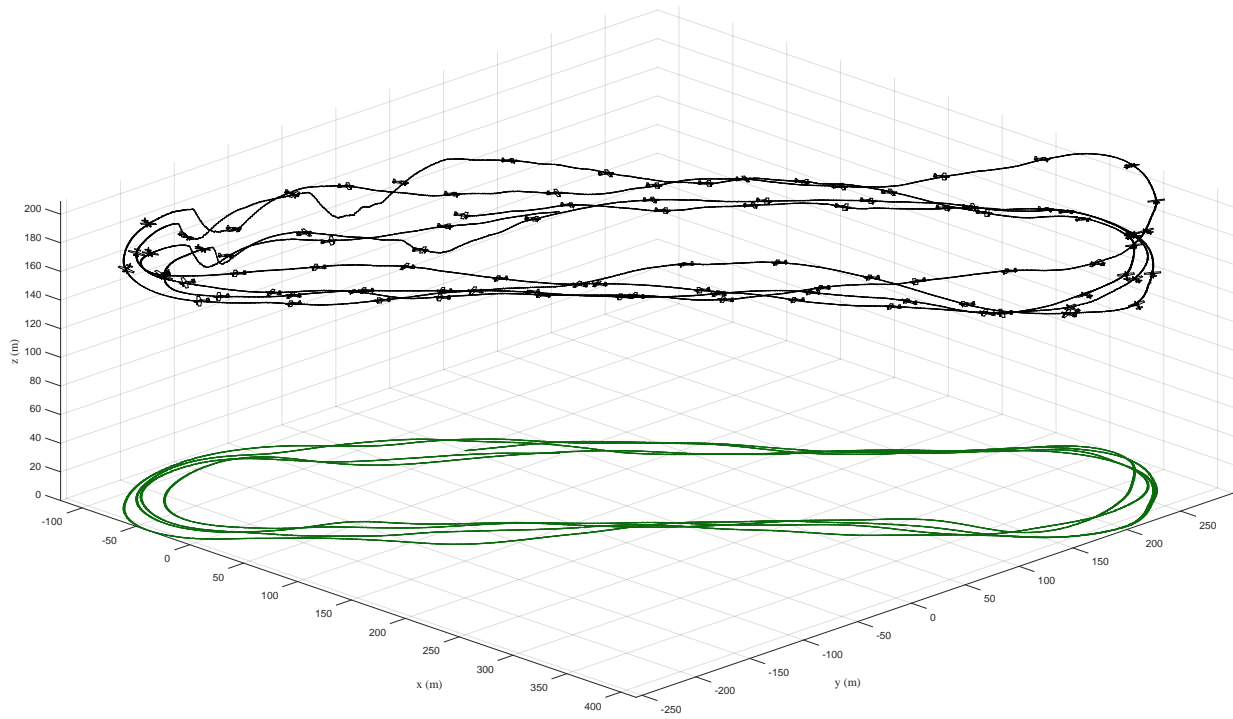


Figure 6: The trajectory of the UIUC-TUM Solar Flyer performing 8 minutes of race tracks within the approximately 1 hour flight under ideal conditions (note that the aircraft is plotted every 5 sec).

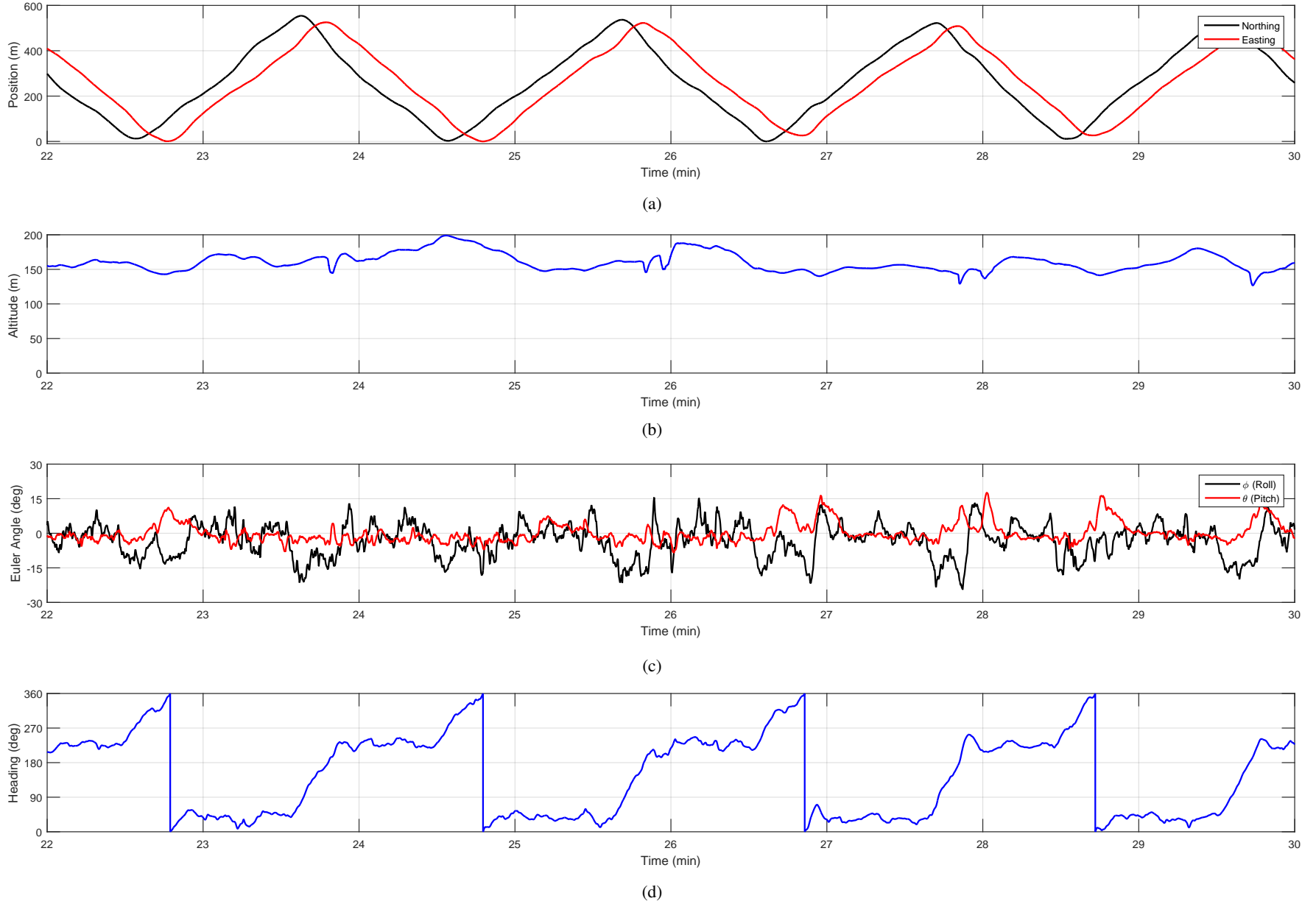
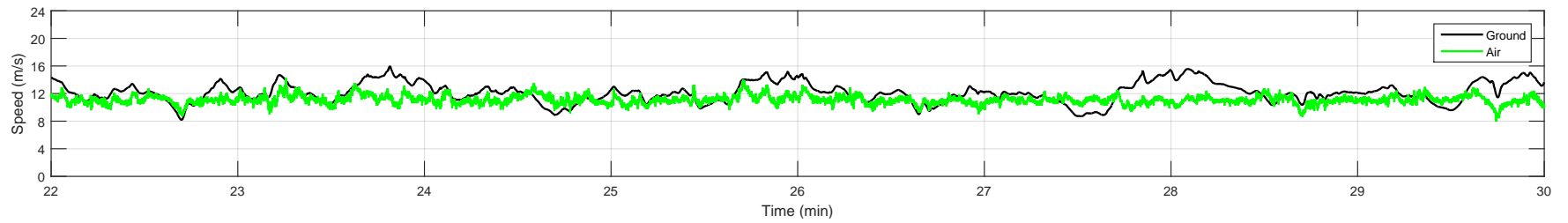
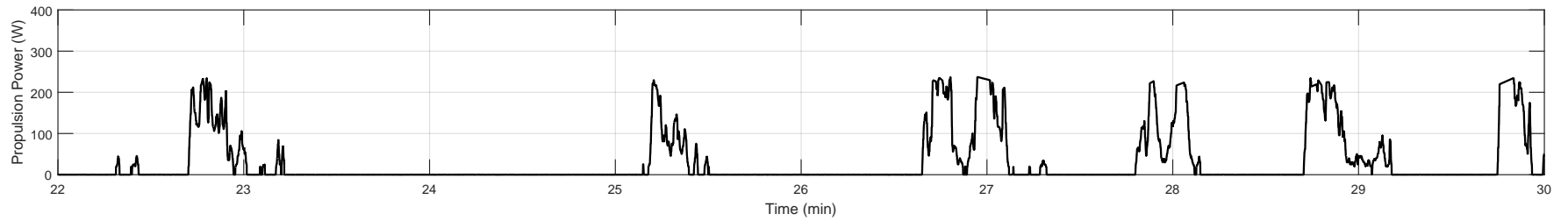


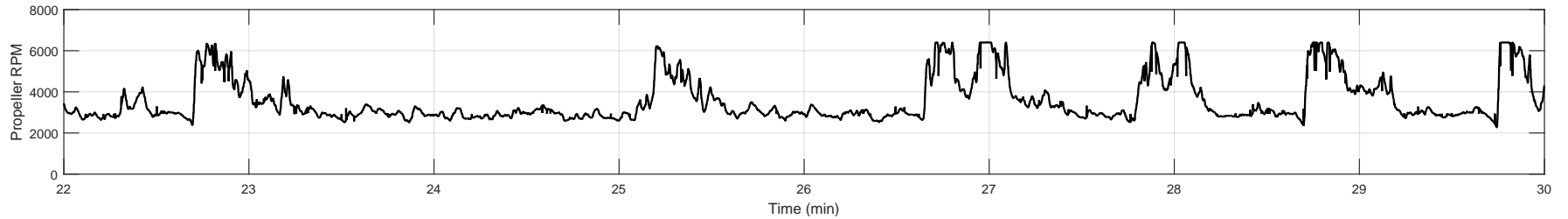
Figure 7: The state data time history of the UIUC-TUM Solar Flyer performing 8 minutes of race tracks within the approximately 1 hour flight under ideal conditions: (a) Northing and Easting position, (b) altitude, (c) pitch and roll, (d) heading.



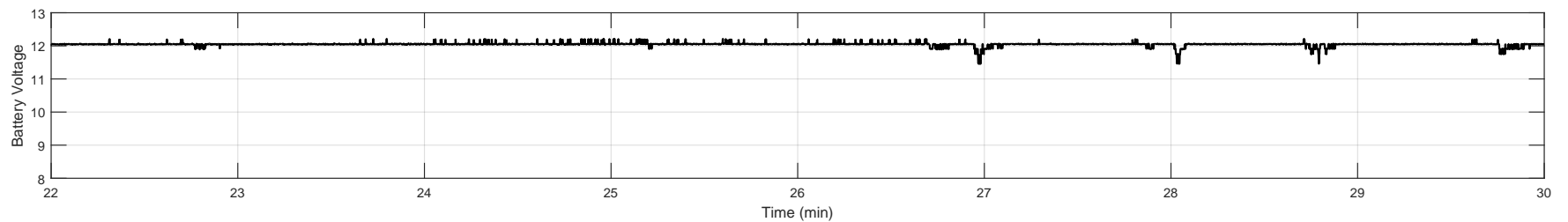
(e)



(f)

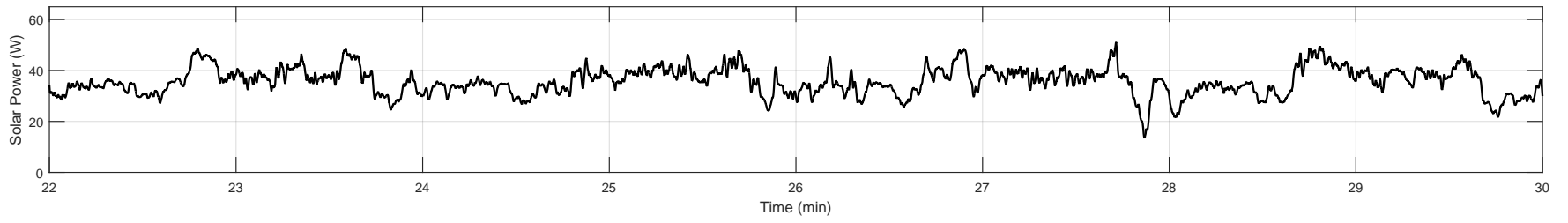


(g)



(h)

Figure 7 (continued): The state data time history of the UIUC-TUM Solar Flyer performing 8 minutes of race tracks within the approximately 1 hour flight under ideal conditions: (e) air and ground speed, (f) propulsion power consumption, (g) propeller rotation rate in RPM, (h) battery voltage.



(i)

Figure 7 (continued): The state data time history of the UIUC-TUM Solar Flyer performing 8 minutes of race tracks within the approximately 1 hour flight under ideal conditions: (i) solar power generated.

B. 8 Hour Flight under Non-Ideal Conditions

An 8 hour flight was performed on August 31, 2020 under non-ideal conditions. The UIUC-TUM Solar Flyer took off at 7:55 AM and landed at 3:59 PM local time. The sun rose at 6:29 AM with an azimuth of 79 deg and set at 7:59pm with an azimuth of 281 deg; solar noon occurring at 1:00pm with an azimuth of 180 deg and an elevation of 59 deg. A nearby national weather station reported that winds were 6-14 mph (2.7-6.3 m/s) shifting from East to the South-West throughout the flight. Additionally, during the flight, the sky coverage was reported as partly-cloudy to cloudy skies, i.e. 50-100% cloud coverage. Locally at the field, the flight crew observed cloudy and hazy skies with the winds of 5-15 mph (2.2-6.7 m/s) with gusts up to 20 mph (8.9 m/s) from East and South (90-180 deg), which was created varying amounts of crosswind with respect to the direction of the the runway and straight legs.

The trajectory of the flight is shown in Fig. 8 with the same perspective as used in the 1 hour flight. As in the other flight, the takeoff was performed on the runway from left to right using a dolly and was followed by an ascent into the same clockwise 650×150 m race track flight pattern. The same altitude of 100 m AGL and airspeed of 11 m/s were maintained and the aircraft performed 188 laps. This was followed by an ascent to landing, which was also performed from left to right on the grass strip parallel to the runway. Using the same equivalency to the aforementioned area coverage mission, the 188 laps were performed during the 478 min of maneuvering, yielding an effective coverage area of 14.1 km² (3,484 acre). Therefore, the race track maneuvering demonstrated during the 8 hour flight with non-ideal conditions equates to an area coverage of 1.8 km²/hr (437 acre/hr), which is a 20% from the 1 hour flight with ideal conditions.

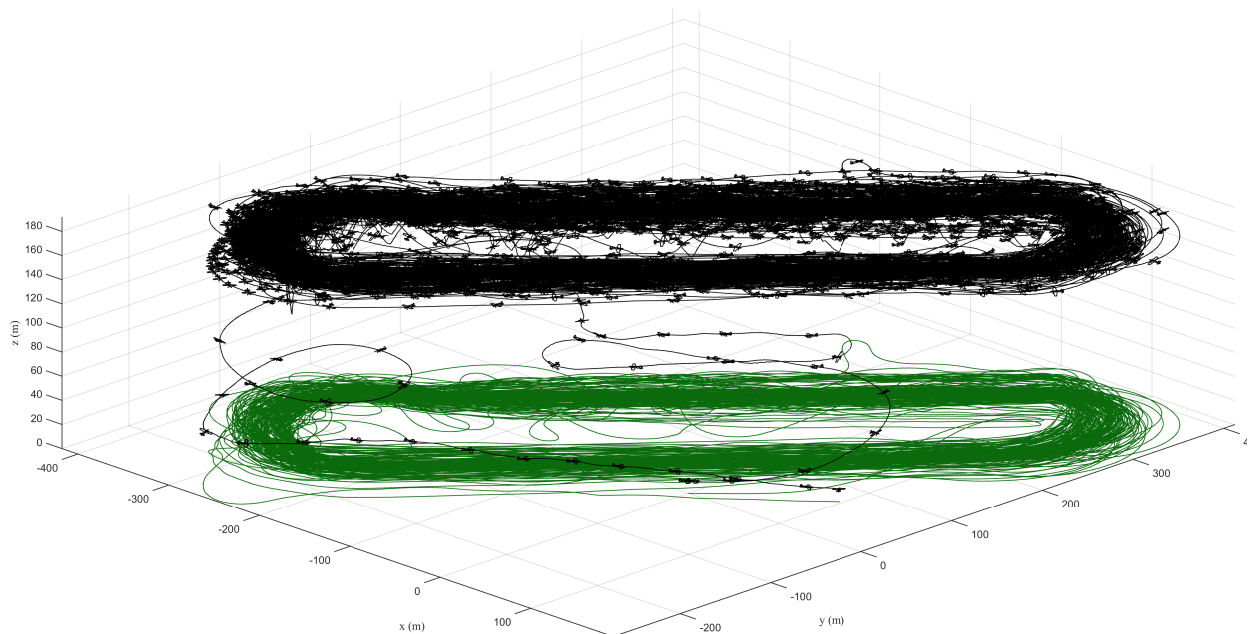


Figure 8: The trajectory of the UIUC-TUM Solar Flyer performing the 8 hour flight under non-ideal conditions (note that the aircraft is plotted every 5 sec).

The flight state data time history is presented in Fig. 9, with similar data being presented in (a)-(i). Additionally, ground (surface) wind speed and direction reported by the nearby national weather station are presented in (j) and (k), respectively. The sky cloud coverage percentage from the same nearby national weather station is presented in (l). Note that the weather reported by the nearby national weather station are an indication of the conditions present at the flight location but do not exactly match. More specifically, the ground winds reported at the weather station, which were measured at 10 m (30 ft) altitude, did not match the wind encountered by the aircraft at 100 m AGL, but are presented to show the overall trend.

Similarly to the other flight, the position and Euler angle data shows 18 race track laps being performed, however, with varied duration averaging approximately 2.5 min long. However, unlike the ideal conditions flight, the vertical excursions present in the 8 hour flight under non-ideal conditions are mostly negative, with larger magnitudes of up to 57 m occurring the middle of the flight. Similar to the other flight, the airspeed data shows an attempt to maintain the 11 m/s commanded airspeed, however, much greater deviations in airspeed occurred, mostly during the middle of the flight, as low as 7 m/s and as high as 16 m/s. During the middle of the flight, the ground speed measured was as low as 1 m/s or as high as 24 m/s, indicating the winds aloft likely exceeded the commanded airspeed, up to approximately 13 m/s. With the large deviations in airspeed, the aircraft attitude also exhibited increased oscillations and overshoots about roll, pitch, and yaw in comparison to the ideal conditions flight. Overall the apparent winds and turbulence aloft presented a significant challenge to the aircraft and autopilot, which they were able to mitigate.

As a result of the more challenging flight conditions encountered, it is visually apparent that the propulsion system consumed additional power than was required on the ideal conditions day, with the greater density of motor-on runs. During the 478 min of maneuvering, the propulsion system consumed an average of 44.6 W, with the majority of the runs occurring during the middle of the day, corresponding to the higher wind and turbulence conditions. However, due to the cloudy conditions present, the solar energy collected could not provide sufficient power to balance the power being consumed by the propulsion system. The solar power can be seen increasing from the launch (1.5 hours after sunrise) up to about 280 min of flight (20 min before solar noon); the power seemed to increase slowly but steadily, with sporadic high solar power collections corresponding to brief moments of direct sunlight. However, at the 280 min of flight, the cloud density at the flight site increased, causing an overall decrease in solar power. As before, some momentary power spikes occurred. During the 478 min of maneuvering, the solar arrays were therefore only able to collect an average of 24.5 W. Thus, due to the non-ideal environmental conditions, the imbalance of solar energy captured and propulsion power required led to the battery being completely discharged over the 8 hour flight.

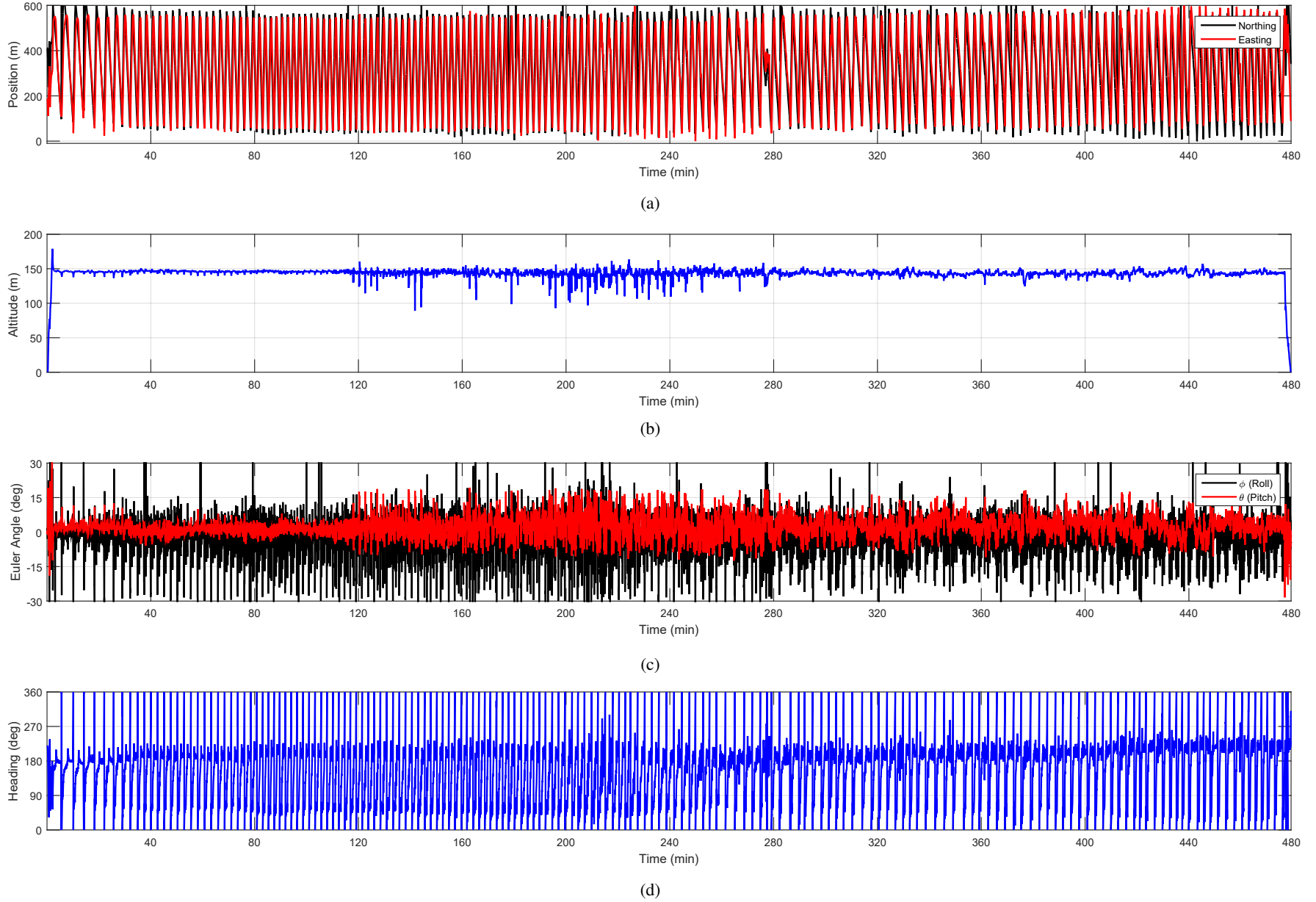
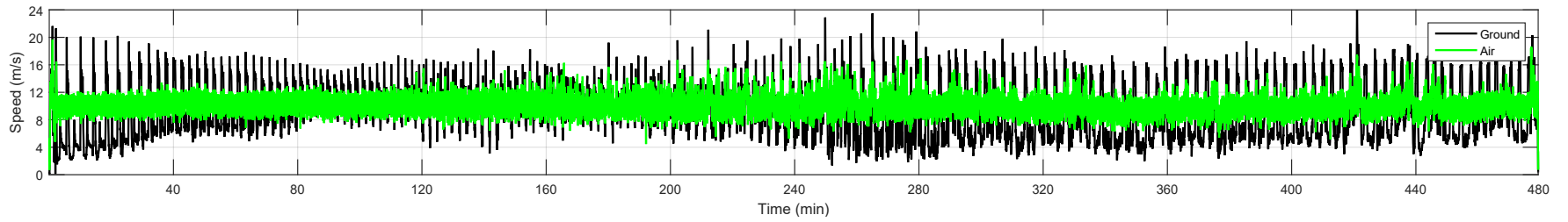
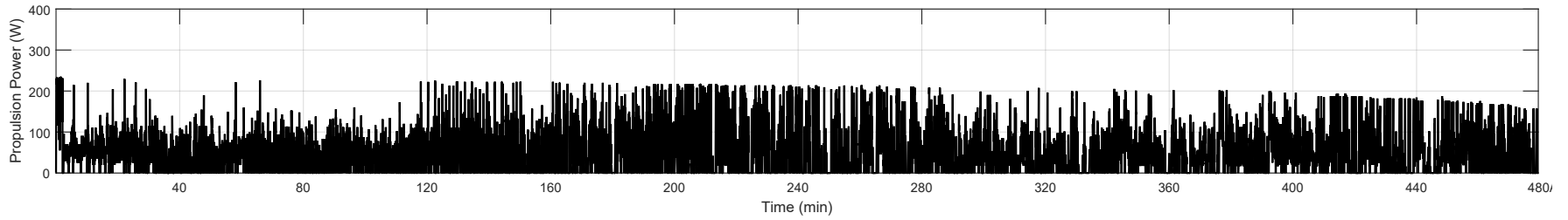


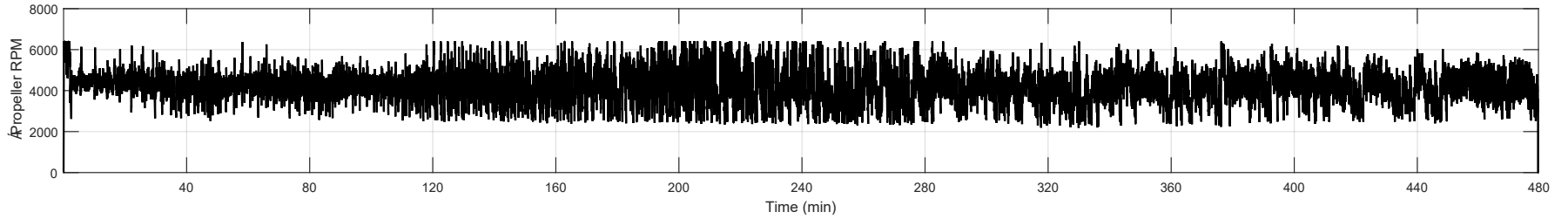
Figure 9: The state data time history of the UIUC-TUM Solar Flyer performing the 8 hour flight under non-ideal conditions: (a) Northing and Easting position, (b) altitude, (c) pitch and roll, (d) heading.



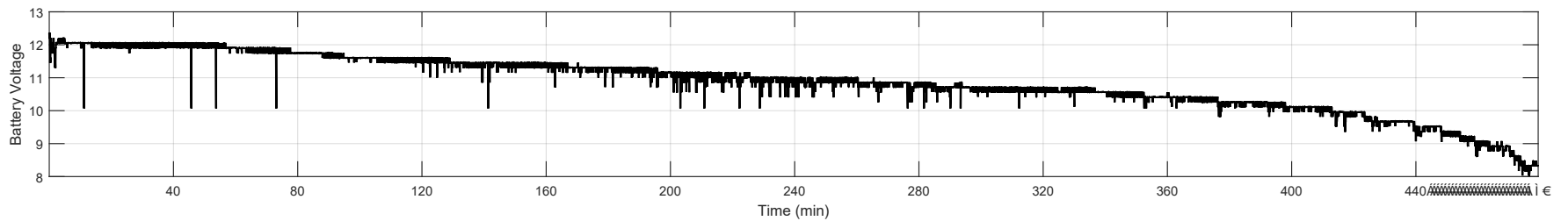
(e)



(f)

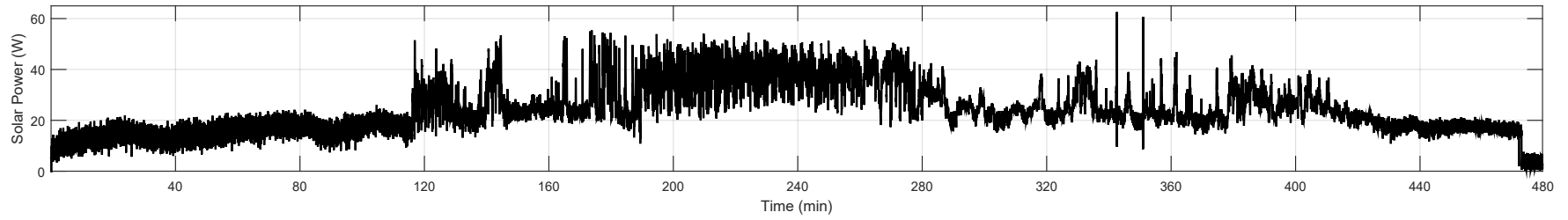


(g)

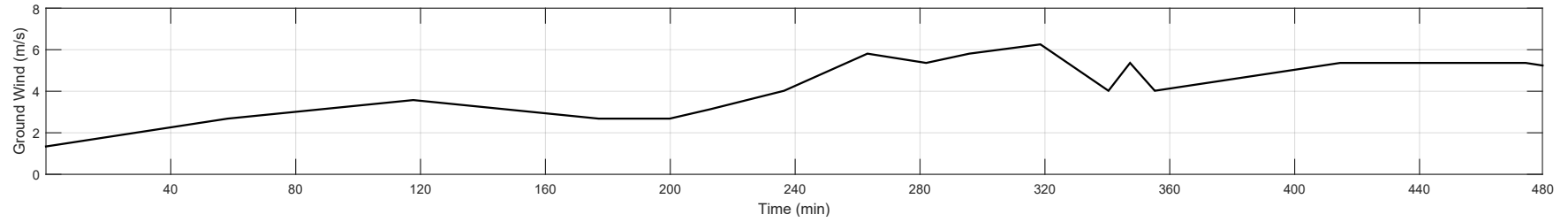


(h)

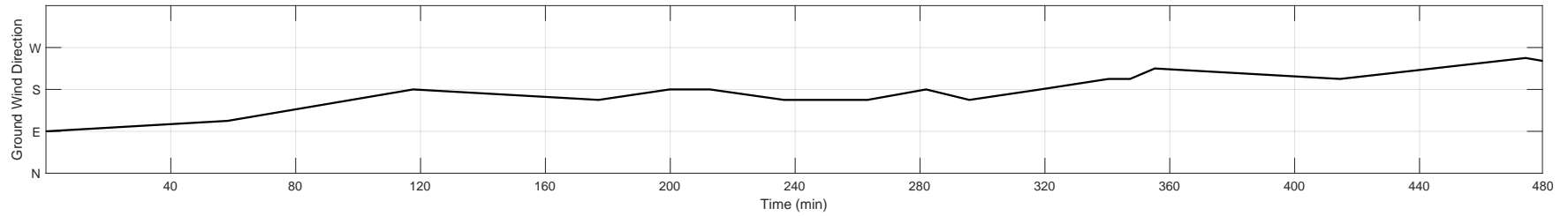
Figure 9 (continued): The state data time history of the UIUC-TUM Solar Flyer performing the 8 hour flight under non-ideal conditions: (e) air and ground speed, (f) propulsion power consumption, (g) propeller rotation rate in RPM, (h) battery voltage.



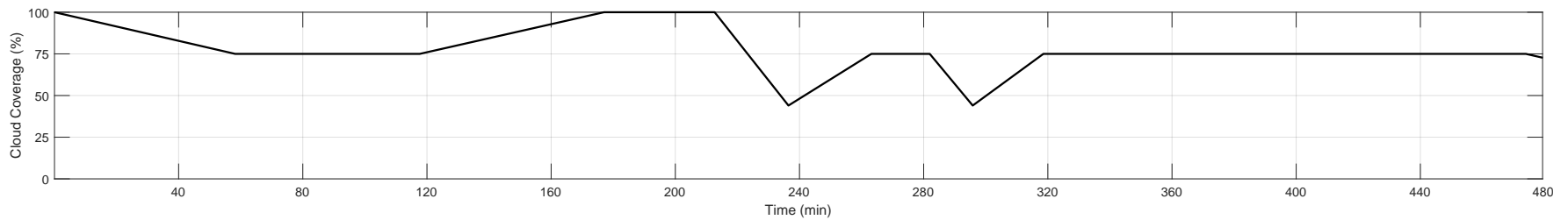
(i)



(j)



(k)



(l)

Figure 9 (continued): The state data time history of the UIUC-TUM Solar Flyer performing the 8 hour flight under non-ideal conditions: (i) solar power generated, (j) ground wind reported, (k) ground wind direction reported, (l) cloud coverage reported.

IV. Conclusions

This paper presented the long-endurance flight testing results of the UIUC-TUM Solar Flyer from the Summer and Fall of 2020. Specifically, the aircraft performed an approximately 1 hour flight under near ideal conditions, and an 8 hour flight under non-ideal conditions. The approximately 1 hour flight showed that under ideal sunny and low-wind conditions, the power consumed by the propulsion and other aircraft systems is balanced with power generated by the solar arrays—this balance was apparent by the constant battery voltage throughout the 1 hour long flight. The 8 hour flight showed that even in rather non-ideal conditions, with high wind and turbulence, increasing the propulsion power consumption, and with high cloud cover, decreasing solar power generation; the aircraft was still able to maintain flight for 8 hours.

Therefore, by joining the results of these two notable flights, it was concluded that under ideal or near-ideal conditions, the UIUC-TUM Solar Flyer would be able to sustain flight from sunrise to sunset and have energy left to support mission systems and sensors. Additionally, given the fact that the approximately 1 hour flight occurred on Oct 8, where the sun only peaks at 46 deg elevation, compared to the yearly average peak of 50 deg and maximum peak of 70 deg on the summer solstice (for 40 deg Latitude), all day flight would be possible from March through October. During the fall and spring months, the UIUC-TUM Solar Flyer could trade some flight time for additional mission power. Meanwhile, during the summer, the aircraft would have surplus energy that could be allocated to more power hungry mission systems and sensors, or could be used to extend flight time into the night if needed.

V. Future Work

In future work, a full-day flight under ideal conditions is planned to demonstrate the aircraft capabilities to balance power consumption and solar power generation with energy storage, and therefore enabling on-board data processing. Further enhancement of the UIUC-TUM Solar Flyer is also planned with better modeling of the batteries and power transmission components. Additionally, to improve the platform, integrating thermal soaring into the flight controller will be beneficial. Furthermore, mission components such as high-resolution visible and infrared cameras are planned to be integrated into the aircraft to enable future demonstrations of the capabilities of the UIUC-TUM Solar Flyer.

When equipped with mission components, the Solar Flyer will be used to perform different missions, ranging from mapping and surveying to agricultural analysis. When performing these missions, trajectory and control optimization will be essential. Due to the high non-linearities, the optimization will likely be non-convex and thus not analytically solvable. Therefore, advanced optimization techniques will be used, among others, reinforcement learning. For applications, coverage path planning and path planning will be considered for wireless data harvesting, which was previously demonstrated in grid world environments.³⁵ The presented eco-system consisting of the flight hardware, uavAP, and uavEE will be valuable to evaluate the applicability of reinforcement learning in this context. Utilizing simulation training, together with curriculum learning to train a reinforcement learning agent for an actual cyber-physical system will be investigated.

Acknowledgments

The material presented in this paper is based upon work supported by the National Science Foundation (NSF) under grant number CNS-1646383 and by the Center for Digital Agriculture (CDA) at the University of Illinois at Urbana-Champaign under a seed funding award. Marco Caccamo was also supported by an Alexander von Humboldt Professorship endowed by the German Federal Ministry of Education and Research. Any opinions, findings, and conclusions or recommendations expressed in this publication are those of the authors and do not necessarily reflect the views of the NSF or CDA.

References

- ¹Precision Hawk, "Precision Agriculture, Commercial UAV and Farm Drones For Sale," <http://precisionhawk.com/>, Accessed Apr. 2015.
- ²MicroPilot, "MicroPilot - MP-Vision," <http://www.micropilot.com/products-mp-visione.htm>, Accessed Apr. 2015.
- ³AeroVironment Inc., "Quantix," <https://www.avdroneanalytics.com/quantix/>, Accessed Dec. 2019.
- ⁴Pix4D SA, "Pix4D," <https://www.pix4d.com/>, Accessed Dec. 2019.
- ⁵Reconstruct Inc., "Reconstruct," <https://www.reconstructinc.com/>, Accessed Dec. 2019.
- ⁶Noth, A., *Design of Solar Powered Airplanes for Continuous Flight*, Ph.D. thesis, ETH Zurich, 2008.
- ⁷Oetershagen, P. et al., "Design of small hand-launched solar-powered UAVs: From concept study to a multi-day world endurance record flight," *Journal of Field Robotics*, Vol. 34, 2017, pp. 1352–1377.
- ⁸Real Time and Embedded System Laboratory, University of Illinois at Urbana-Champaign, "Solar-Powered Long-Endurance UAV for Real-Time Onboard Data Processing," <http://rtsl-edge.cs.illinois.edu/UAV/>, Accessed Jan. 2018.
- ⁹Dantsker, O. D., Theile, M., and Caccamo, M., "Design, Development, and Initial Testing of a Computationally-Intensive, Long-Endurance Solar-Powered Unmanned Aircraft," AIAA Paper 2018-4217, AIAA Applied Aerodynamics Conference, Atlanta, Georgia, Jun. 2018.
- ¹⁰"F5 Models," <http://f5models.com>, Accessed Oct. 2017.
- ¹¹Ahn, I.-Y., Bae, J.-S., Park, S., and Yang, Y.-M., "Development and Flight Test of a Small Solar Powered UAV," Vol. 41, 11 2013.
- ¹²Ahn, I.-Y., Yang, Y.-M., Ju, Y.-C., Park, S., and Bae, J.-S., "Efficiency Estimation on Propulsion System of an Electric Powered UAV," Vol. 23, 09 2015, pp. 1–7.
- ¹³"Top Model CZ," <https://www.topmodelcz.cz/>, Accessed Oct. 2017.
- ¹⁴Dantsker, O. D., Imtiaz, S., and Caccamo, M., "Electric Propulsion System Optimization for Long-Endurance and Solar-Powered Unmanned Aircraft," AIAA Paper 2019-4486, 2019 AIAA/IEEE Electric Aircraft Technologies Symposium, Indianapolis, Indiana, Aug. 2019.
- ¹⁵Dantsker, O. D., Deters, R. W., and Caccamo, M., "Propulsion System Testing for a Long-Endurance Solar-Powered Unmanned Aircraft," AIAA Paper 2019-3688, AIAA Applied Aerodynamics Conference, Dallas, Texas, Jun. 2019.
- ¹⁶Dantsker, O. D., Theile, M., and Caccamo, M., "A High-Fidelity, Low-Order Propulsion Power Model for Fixed-Wing Electric Unmanned Aircraft," AIAA Paper 2018-5009, AIAA/IEEE Electric Aircraft Technologies Symposium, Cincinnati, OH, Jul. 2018.
- ¹⁷Drela, M., "First-Order DC Electric Motor Model," http://web.mit.edu/drela/Public/web/qprop/motor1_theory.pdf.
- ¹⁸Oi, M., Zeune, C., and Logan, M., "Analytical/Experimental Comparison for Small Electric Unmanned Air Vehicle Propellers," *26th AIAA Applied Aerodynamics Conference*, American Institute of Aeronautics and Astronautics, Reston, Virginia, 8 2008.
- ¹⁹Dantsker, O. D., Caccamo, M., Deters, R. W., and Selig, M. S., "Performance Testing of Aero-Naut CAM Folding Propellers," AIAA Paper 2020-2762, AIAA Aviation Forum, Virtual Event, Jun. 2020.
- ²⁰Brandt, J., Deters, R., Ananda, G., Dantsker, O., and Selig, M., "UIUC Propeller Database," <http://m-selig.ae.illinois.edu/props/propDB.html>.
- ²¹O. Dantsker and R. Mancuso and M. Vahora and M. Caccamo, "Unmanned Aerial Vehicle Database," <http://uavdb.org/>.
- ²²Dantsker, O. D., Caccamo, M., and Imtiaz, S., "Propulsion System Design, Optimization, Simulation, and Testing for a Long-Endurance Solar-Powered Unmanned Aircraft," AIAA Paper 2020-3966, AIAA Propulsion and Energy 2020 Forum, Virtual Event, Aug. 2020.
- ²³Hacker Motor GmbH, "Hacker Brushless Motors," <https://www.hacker-motor.com/>, Accessed Aug. 2020.
- ²⁴Model motors s.r.o., "AXI Model Motors," <http://www.modelmotors.cz/>, Accessed Jun. 2021.
- ²⁵Neutronics, "NeuMotors," <https://neumotors.com/>, Accessed Aug. 2020.
- ²⁶Dantsker, O. D., Theile, M., and Caccamo, M., "Integrated Power Modeling for a Solar-Powered, Computationally-Intensive Unmanned Aircraft," AIAA Paper 2020-3568, AIAA/IEEE Electric Aircraft Technologies Symposium, Virtual Event, Aug. 2020.
- ²⁷Al Volo LLC, "Al Volo: Flight Systems," <http://www.alvolo.us>, Accessed Aug. 2020.
- ²⁸Dantsker, O. D. and Mancuso, R., "Flight Data Acquisition Platform Development, Integration, and Operation on Small- to Medium-Sized Unmanned Aircraft," AIAA Paper 2019-1262, AIAA SciTech Forum, San Diego, California, Jan 2019.
- ²⁹Mirco Theile, "uavAP: A Modular Autopilot for Unmanned Aerial Vehicles," <https://github.com/theilem/uavAP>.
- ³⁰Theile, M., Dantsker, O. D., Caccamo, M., and Yu, S., "uavAP: A Modular Autopilot Framework for UAVs," AIAA Paper 2020-3268, AIAA Aviation 2020 Forum, Virtual Event, Jun. 2020.
- ³¹Mirco Theile, "uavGS: A Modular Ground Control Station Interface for Unmanned Aerial Vehicles," <https://github.com/theilem/uavGS>.
- ³²Theile, M., Dantsker, O. D., Nai, R., and Caccamo, M., "uavEE: A Modular, Power-Aware Emulation Environment for Rapid Prototyping and Testing of UAVs," IEEE International Conference on Embedded and Real-Time Computing Systems and Applications, Hakodate, Japan, Aug. 2018.
- ³³Dantsker, O. D., Theile, M., Caccamo, M., Yu, S., and Vahora, M., "Continued Development and Flight Testing of a Long-Endurance Solar-Powered Unmanned Aircraft: UIUC-TUM Solar Flyer," AIAA Paper 2020-0781, AIAA SciTech Forum, Orlando, Florida, Jan. 2020.
- ³⁴Dantsker, O. D., Theile, M., and Caccamo, M., "A Cyber-Physical Prototyping and Testing Framework to Enable the Rapid Development of UAVs," *Submitted to Aerospace*, 2021.
- ³⁵Theile, M., Bayerlein, H., Nai, R., Gesbert, D., and Caccamo, M., "UAV Path Planning using Global and Local Map Information with Deep Reinforcement Learning," *arXiv preprint arXiv:2010.06917, Submitted to 2021 IEEE/RSJ International Conference on Intelligent Robots and Systems (IROS)*, 2020.